

# Incorporation of silver in DyBa<sub>2</sub>Cu<sub>3</sub>O<sub>7- $\delta$</sub> ceramics. Correlation between superconducting properties and microstructure

C Nguyen-van-Huong, E Crampin, J Y Laval and A Dubon

Laboratoire de Physique du Solide, CNRS ESPCI, 10 rue Vauquelin, 75231 Paris Cedex 05, France

Received 30 July 1996, in final form 6 November 1996

**Abstract.** The incorporation of silver in DyBCO ceramics was studied by EDX in TEM and correlated with the superconducting properties through  $R-T$ ,  $I-V$  characteristics and critical current as a function of an external magnetic field. Two types of doping were performed: addition (A samples) and substitution (S samples) for  $0 \leq x \leq 0.4$ . It was observed that for A samples,  $T_c$  increases by  $\approx 2$  K and  $J_c$  is improved by a factor of 2. The influence of the applied field ( $B \leq 30$  G) upon  $J_c$  decreases slightly with  $x$  for A samples but the weak link behaviour remains. It was shown that silver does not enter in the 123 lattice. It slightly segregates at grain boundaries maintaining narrow junctions which are likely improve the coupling between grains, explaining the observed increase in  $J_c$ . On the contrary, for S samples,  $T_c$  is unchanged and the transition is wider. The effect of the magnetic field on  $J_c$  increases with the doping level. Silver is found in the lattice, but the concentration is always lower than the nominal one and is limited to 0.12 for  $x = 0.4$ . This limited solubility leads to a deficiency in copper and consequently to noticeable ratio of second phases. Furthermore, a high segregation was observed at grain boundaries. This specific microstructure which produces wider junctions explains the decrease in  $J_c$ .

## 1. Introduction

Since the discovery of new high-temperature superconductors, much attention has been paid to studying the role of silver in YBCO material [1–11]. These investigations have led to a significant improvement in the properties of YBCO ceramics. In particular, addition of silver increases the grain size, texturation and homogeneity [12–14] and enhances the critical temperature and the current density. It reduces the normal state resistivity in bulk material [2, 12, 14, 15] as well as in thin films [16, 17]. However, some works have shown that the critical density is unchanged [4, 5, 7, 15] or decreased [6, 17]. In summary, silver seems to play either a positive or a negative role in the improvement of the superconducting properties of YBCO depending on the silver content in the sample and processing conditions.

Furthermore, study of the distribution of Ag in ceramic materials is also subject to contradictory conclusions. There is some agreement about the presence of Ag in voids and grain boundaries but the presence of Ag in the YBCO lattice is still questionable. Some authors have reported that Ag does not diffuse into the grains [3, 18] but most authors stated in contrast that Ag exhibits some solubility in YBCO and substitutes for Cu [8–11, 19, 20].

In this paper attempts to shed light on the effect of silver on the superconducting properties of DyBCO as a function of the type of doping, addition (DyBa<sub>2</sub>Cu<sub>3</sub>O<sub>7- $\delta$</sub> -Ag <sub>$x$</sub> ) or substitution (DyBa<sub>2</sub>Cu<sub>3- $x$</sub> Ag <sub>$x$</sub> O <sub>$y$</sub> ), and to correlate them with the microstructure of the materials. In particular, chemical microanalysis by EDX in TEM allowed us to track the amount of silver in grain boundaries and within the grains. This amount depends strongly on the kind of sample, whether Ag is added to already synthesized DyBa<sub>2</sub>Cu<sub>3</sub>O<sub>7- $\delta$</sub>  (A) or to the starting powder (C) or is assumed to substitute for Cu (S).

## 2. Experiment

The materials with doping level  $0 \leq x \leq 0.4$  were prepared by the usual solid state reaction method. In the first type of sample DyBa<sub>2</sub>Cu<sub>3</sub>O <sub>$y$</sub> -Ag <sub>$x$</sub> , silver was added as Ag<sub>2</sub>O either to already synthesized DyBa<sub>2</sub>Cu<sub>3</sub>O<sub>7- $\delta$</sub>  (A) or incorporated at the beginning of the synthesis with the other components (high-purity Dy<sub>2</sub>O<sub>3</sub>, CuO, BaCO<sub>3</sub>) in stoichiometric ratio (C). In the second type (DyBa<sub>2</sub>Cu<sub>3- $x$</sub> Ag <sub>$x$</sub> O <sub>$y$</sub> ), Ag was considered as a substituent for Cu. The different powders were mixed in a mortar and pressed into pellets. They were fired three times at 920 °C in air for 10 h with

intermediate grinding, mixing and pressing in order to complete the reaction and to improve the homogeneity of the materials. They were then sintered under an oxygen atmosphere by heating at 980 °C for 100 h and finally oxygenated at 500 °C for 4 h and furnace-cooled to ambient temperature. These conditions were found to give the largest grains and the most homogeneous microstructure. It was observed that for (C) samples the presence of silver tended to lower the melting point of the mixture, contrary to (A) and (S) samples. Each batch of samples with variable  $x$  underwent the heat treatment at the same time, thus under rigorously identical conditions. This procedure allowed the change in the properties of the materials to be unambiguously attributed to the doping and not to the processing conditions.

The phases were characterized by powder x-ray diffraction (XRD) using a Philips automated x-ray diffractometer. For transmission electron microscopy (TEM) and EDX microanalysis the samples were thinned by mechanical polishing with alumina paper down to a thickness of 20–30  $\mu\text{m}$ , then by  $\text{Ar}^+$  milling down to electronic transparency (50 nm or less). Microstructural and compositional analyses were performed with a Jeol 2000 FX TEM equipped with a Link EXL x-ray selective analyser and in a SEM equipped with an EDAX x-ray selective analyser.

The superconducting properties were studied by measuring the electrical resistivity–temperature ( $R$ – $T$ ) and current–voltage ( $I$ – $V$ ) characteristics which were carried out with a conventional d.c. four-probe configuration. The electrical contacts were made with silver paint fired at 400 °C for 1 h in flowing oxygen. The transport current density was determined at 77 K, with and without external magnetic field, from the current–voltage curves. The external magnetic field, supplied by two Helmholtz copper coils, ranged from 0 to 40 G and was perpendicular to the sample surface. The 1  $\mu\text{V}$  criterion was applied to determine the critical current value. The critical temperature  $T_c$  was deduced from the  $R$ – $T$  curves and defined as the temperature for which  $R = 0$ . Magnetic screening measurements were made to estimate the superconducting volume.

### 3. Results and discussion

#### 3.1. XRD

XRD patterns show well defined peaks which are indexable as the orthorhombic  $\text{DyBa}_2\text{Cu}_3\text{O}_{7-\delta}$  unit cell. For Ag content  $x \leq 0.1$ , all the samples are single phase and no noticeable peak corresponding to a second phase or metallic Ag is detectable. For  $x > 0.1$ , the XRD patterns indicate the presence of metallic Ag phase and non-superconducting phases such as  $\text{Dy}_2\text{BaCuO}_5$  ‘211’,  $\text{BaCuO}_2$  ‘011’ and CuO. These second phases were notable only for (S) samples. Their amount increases with increasing Ag content (figure 1). Moreover the reflection lines appear to be slightly broadened for S samples indicating a less crystallized materials. In this case, since it is expected to replace Cu by Ag, no impurity phase

should be encountered as long as Ag goes into the Cu sites, no impurity phase should be expected. As soon as the solubility limit is exceeded, the situation becomes similar to the case of a Cu-deficient composition. According to the phase diagram, a deficiency in copper should give rise to ‘211’ and ‘011’ impurity phases. Therefore the appearance of a perceptible amount of ‘211’ and ‘011’ phases could indicate the value of the solubility limit of Ag. It will be shown further that the value observed by XRD, which is situated around  $x = 0.1$ , is generally not overestimated.

The  $a$ ,  $b$ ,  $c$  lattice parameters calculated from the (200), (020) and (006) reflection lines are represented as a function of Ag content for added (A) and for substituted (S) samples in figure 2. For (A) and (C) samples, one can notice that the lattice parameters increase very slightly up to  $x = 0.2$  then decrease and become similar to those obtained on undoped samples, but these changes are very small and within the limit of accuracy of the method. In (S) samples, the  $a$  parameter is unchanged while  $b$  and  $c$  decrease slightly for  $x \geq 0.2$ . This evolution of  $b$  and  $c$  parameters is consistent with the resulting Cu deficiency found in these samples when the amount of Ag replacing Cu is less to the nominal one. In order to confirm this effect,  $\text{DyBa}_2\text{Cu}_{3-x}\text{O}_{7-\delta}$  samples with  $x = 0.2$  and 0.4 were synthesized and their lattice parameters determined. Effectively, similar changes in  $b$  and  $c$  axes were observed and no variation for the  $a$  parameter was found. For samples where Ag is added, an increase in  $c$  axis was usually reported [3, 20, 21] whereas for substituted samples, Weinberger *et al* [10] claimed a minute increase of the lattice parameters while Taylor and Greaves [19] stated a decrease in the  $c$  axis.

#### 3.2. Optical microscopy and SEM

Samples with various nominal silver concentrations were submitted to dry polishing. The surfaces were observed by scanning electron microscopy. Undoped samples exhibited platelet-like grains with an average thickness of 20  $\mu\text{m}$  and an average length of 40–50  $\mu\text{m}$  (figure 3). The effect of silver on the microstructure depends strongly on the type of doping, i.e. addition or substitution. In the first case, no significant change could be found. For substituted samples, the modification is important: the grains are squarer and smaller, and for high silver content,  $x \geq 0.2$ , the grain shape is complicated. For high doping level, some bright second phases and intergranular phases corresponding to metallic Ag can be discerned.

#### 3.3. Superconducting properties

The change in the superconducting properties of DyBCO arising from the presence of silver also differs with the doping type, i.e. addition (A and C samples) or substitution (S samples).

For (A) samples, the presence of a small amount of silver tends to improve the superconducting behaviour: the resistive transition is slightly steepened and the critical temperature is enhanced by  $\approx 2$  K (figure 4). For  $x > 0.2$ ,  $T_c$  is similar to that obtained with undoped samples. In the

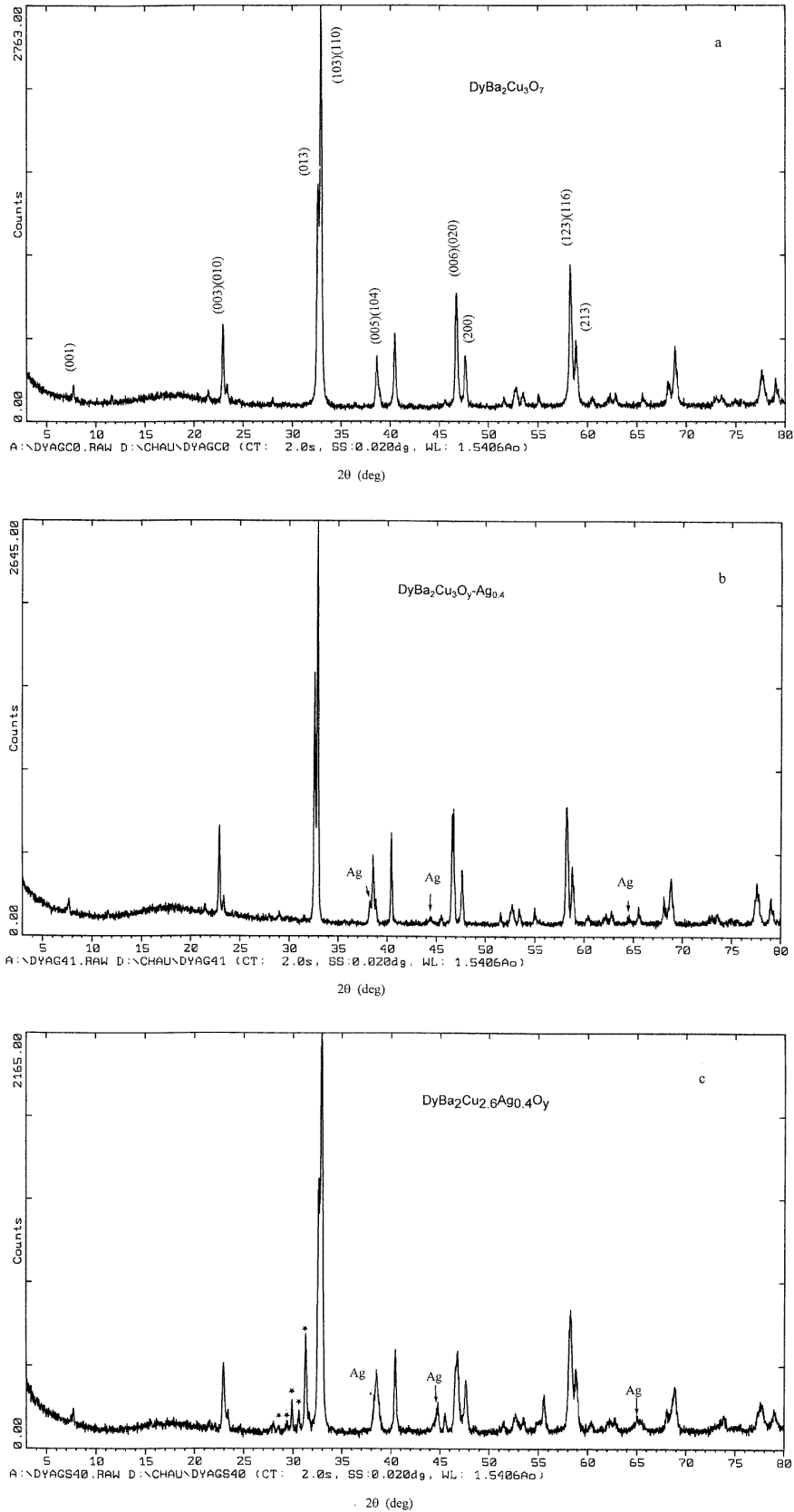


**Figure 1.** XRD diagrams: (a) non-doped sample; (b) sample A ( $x = 0.4$ ); (c) sample S ( $x = 0.4$ ). The arrows indicate the reflection lines of Ag and (\*) correspond to secondary phases such as Dy<sub>2</sub>BaCuO<sub>5</sub> and BaCuO<sub>2</sub>.

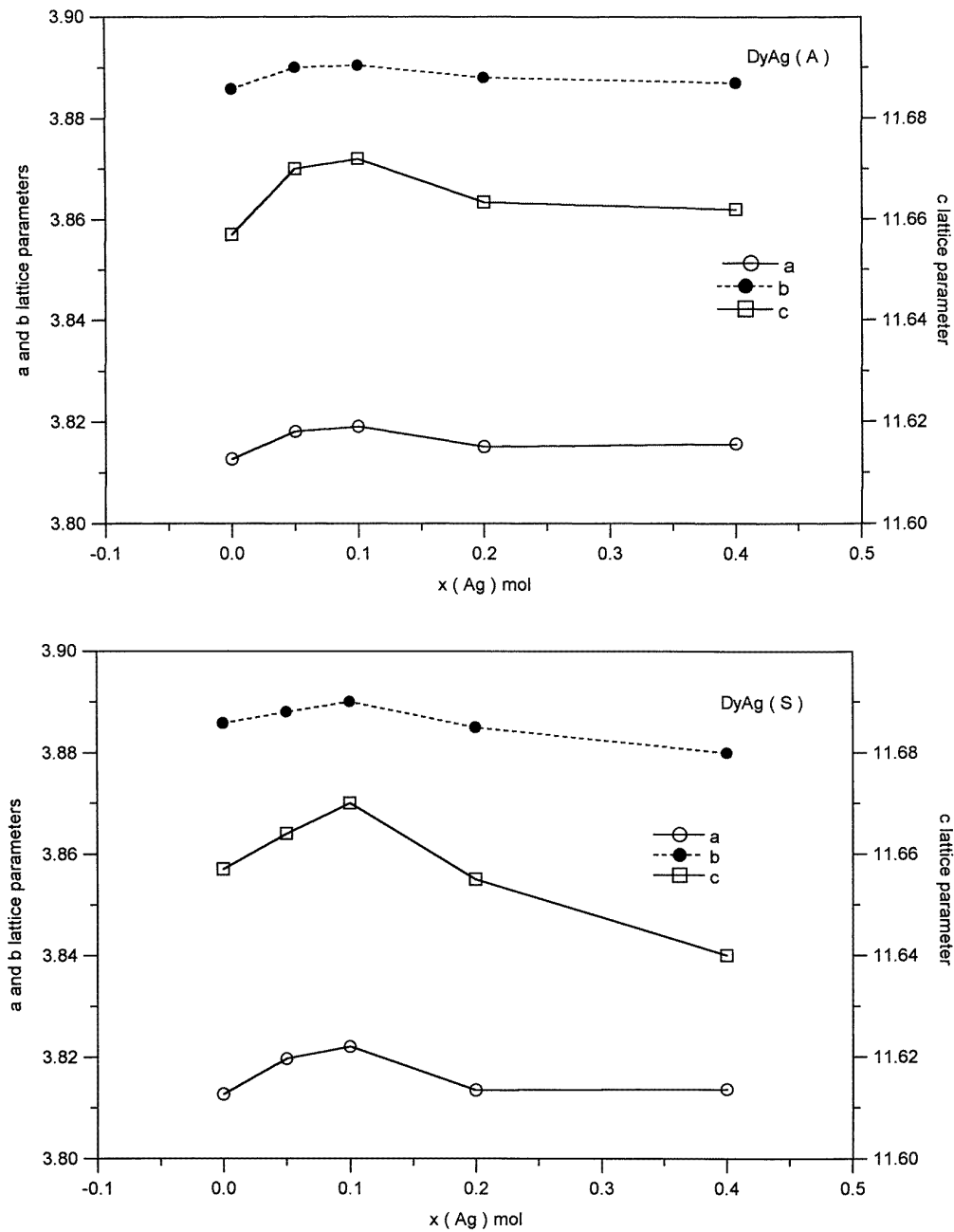


**Figure 2.** Variation of lattice parameters  $a$ ,  $b$  and  $c$  with the doping level  $x$  for A and S samples.

whole range of doping, the normal state resistivity decreases with increasing  $x$  (figure 5). The critical current density  $J_c$  varies from 100 to 250 A cm<sup>-2</sup> for  $x = 0$  and  $x = 0.4$  respectively (figure 6).

For (S) samples, the results are different. The critical temperature is practically unchanged, but the resistive transition tends to be wider ( $\Delta T$  varies from  $\approx 1.5$  to 4.5 K for  $x = 0$  and  $x = 0.4$  respectively). The normal state resistivity increases with  $x$  (figure 5) and the critical current density decreases notably (figure 6). Moreover magnetic measurements show a slight decrease of the superconducting volume with increasing  $x$  (in comparison

with  $x = 0$ , the superconducting volume is only 92% and 84% for  $x = 0.2$  and  $x = 0.4$  respectively).

In figure 7 we have represented the  $I$ - $V$  characteristic for an undoped sample in zero field at 77 K. This characteristic is the same for doped samples. The transition from zero to finite voltage is smooth and the normal state resistance is low ( $\approx 3.5 \times 10^{-4}$   $\Omega$ ). This behaviour is indicative of granular materials [22]. This is in agreement with what was shown [23, 24] on HTSC ceramics prepared by sintering which were described as agglomerates of grains of stoichiometric material separated by layers of non-stoichiometric intergranular material.

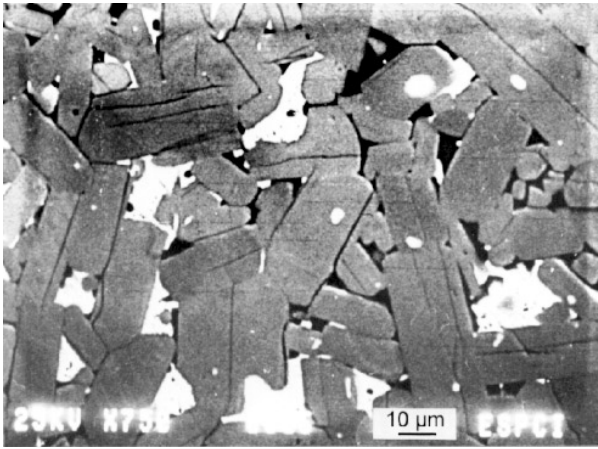


**Figure 3.** SEM micrograph of sample A ( $x = 0.4$ ).

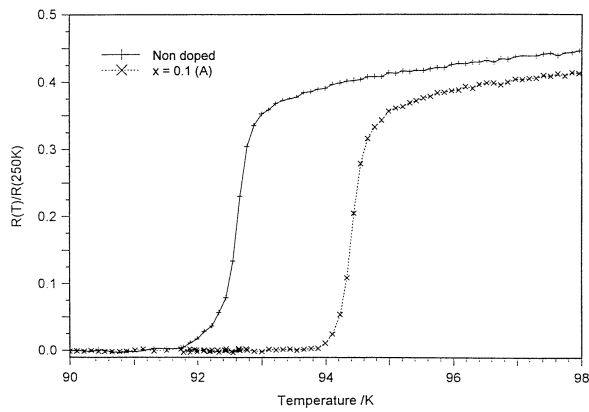


**Figure 4.** Normalized resistance as a function of temperature for non-doped and A ( $x = 0.1$ ) samples.

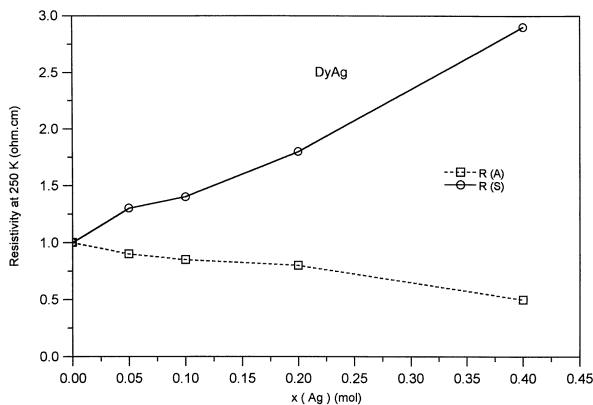


**Figure 5.** Effect of Ag doping on the normal state resistivity of A and S samples.

The effect of an external magnetic field  $B$  on the transport critical current was studied. In figure 8,  $J_c(B)/J_c(0)$  is represented as a function of  $B$  in a log scale. As the field increases ( $0 \leq B \leq 25$  G) the current was found to drop rapidly then reaches a plateau. This behaviour was observed in all the samples studied. In figure 8(a),

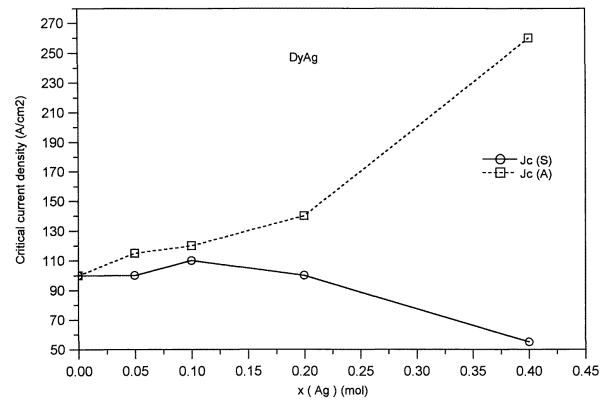


**Figure 6.** Variation of the critical current with Ag doping for A and S samples.

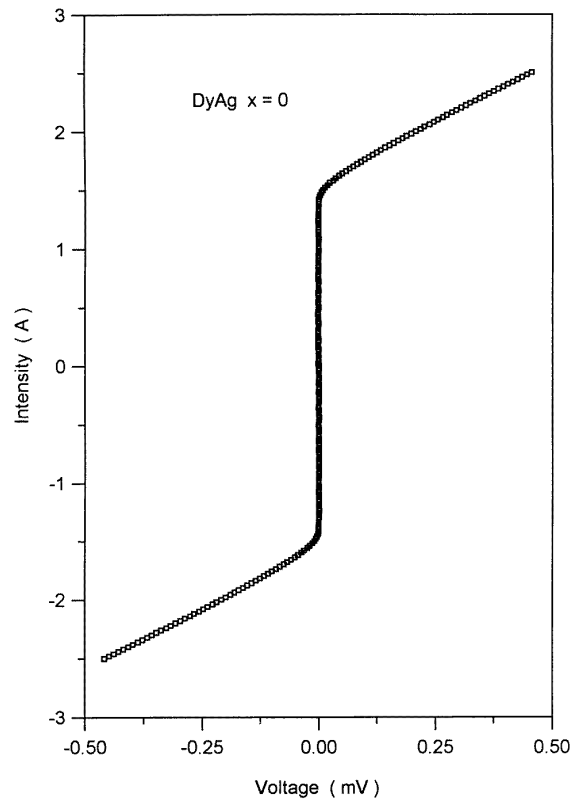


**Figure 7.** Current-voltage characteristic at 77 K of an undoped sample in zero field.

the curve obtained with  $x = 0.4$  A which exhibited the highest  $J_c$  shows the lowest rate of  $J_c$  drop whereas those corresponding to  $x = 0$  and  $x = 0.2$  coincide. In contrast, the 0.2S curve is above the 0.4S one. Qualitatively these curves are similar to those reported in the literature for sintered YBCO in magnetic fields below 50 G [25,26]. In those works, the results were fitted with models assuming that  $J_c$  was limited by weak link junctions (SNS or SIS junction) located at the grain boundaries. At large field, it was found that  $J_c$  varied as  $(B/B_0)^n$  where  $n$  took the values  $-1$  or  $-1.5$  according to the type of the current-

**Table 1.** Exponent  $n$ , cross-sectional area  $dL$  and length  $L$  of the weak link junctions calculated from the  $J_c(B)$  characteristics for A and S samples.

$x$	$n$	$dL$ ( $\mu\text{m}^2$ )	$L$ ( $\mu\text{m}$ )
0	-1.6	11.7	40
0.2A	-1.4	17.7	60
0.4A	-1.2	17	50
0.2S	-1.2	8.6	30
0.4S	-1.5	15	50

field pattern, either Fraunhofer or Airy type respectively. Similarly, here it was considered that for large  $B$

$$J_c(B)/J_c(0) = (B/B_0)^n$$

where  $B_0$  is a characteristic field defined as  $B_0 = \phi_0/dL$ ,  $\phi_0$  is the flux quantum,  $d$  and  $L$  the thickness and length of the junctions.

In table 1 we report the calculated  $n$  and  $L$  values assuming that  $d = 2\lambda$  ( $\lambda$  is the London penetration depth and assumed equal to 150 nm). It is seen that  $n$  varies from  $-1.6$  to  $-1.2$ . The calculated length of the junctions is close to the observed average grain size (see figure 3) except for  $x = 0.4S$  where the grain size ranges from 20 to 30  $\mu\text{m}$ .

At  $B > 10$  G, it can be noted that experimental data lay above the extrapolated curves. This may be attributed, as suggested by Peterson and Ekin [25], to the fact that at these fields, current flow is controlled by percolative phenomena along strong links. Furthermore the plateau observed at  $B > 20$  G occurs at comparable values for all samples but  $I_c(B)/I_c(0)$  is slightly higher for the sample 0.4A.

Thus, for all samples the mechanism controlling  $J_c$  appears identical and the enhancement of  $J_c$  is likely to be attributed to a more favourable distribution of the weak links whose behaviour is related to the microstructure of the grain boundaries (as can be seen below). In a recent paper, Sarma *et al* [27] have shown that grain boundaries in melt-textured Ag-doped  $\text{YBa}_2\text{Cu}_3\text{O}_{7-\delta}$  could behave either as strong or weak links in contrast to non-Ag-doped materials where only weak links were found.

For S samples which present similar  $J_c(B)$  curves, the decrease of  $J_c$  is attributable to a degradation of the weak link behaviour due to the increasing presence of non-superconducting phases acting as a barrier to current flow. In the following, we tried to correlate these effects with the microstructure and especially with the chemical local composition of the samples within grains as well as at grain boundaries.

#### 4. Microanalysis in TEM and in SEM

Localized quantitative chemical analysis was carried out in analytical TEM by EDX. The incident energy of electrons was 200 keV. The spatial resolution was close to the electron beam diameter. For quantitative analysis, to get reliable data, at least 15 large grains of various morphologies were analysed on each sample. An example of an EDX spectrum is given in figure 9.

From EDX results, one can conclude:

(i) In all samples, silver segregates at clean grain boundaries and precipitates at dirty grain boundaries and in triple junctions, but not in the  $\text{BaCuO}_2$  or  $\text{CuO}$  secondary phases.

(ii) Silver was found in grains for substituted samples only and not for samples with Ag addition, and that for all doping levels.

In spite of some scattering in the data, the average concentration of Ag in the grains for  $\text{DyBa}_2\text{Cu}_{3-x}\text{Ag}_x\text{O}_y$  can be calculated for different  $x$  values; the results are reported in table 2. For the most dilute material ( $x = 0.05$ ), no value was given since the amount is under the limit of detection (0.03). For  $x = 0.1$ , a noticeable proportion of grains did not exhibit any detectable Ag concentration ( $< 0.03$ ), the reported value corresponds to an average of the significant values. For  $x \geq 0.2$ , the distribution of Ag in the grains is more homogeneous.

It can be noted in table 2 that the percentage of silver measured by EDX in the grains increases with  $x$  but is systematically smaller than the nominal one. It seems to saturate at about 0.1–0.12; the remaining part is found in metallic Ag precipitates and in second phases which are located at grain boundaries and triple junctions. Since there are a significant number of unoccupied Cu sites which are not replaced by silver, the resulting effect is quite similar to the behaviour found on a material with a deficiency in Cu: grains of composition close to  $\text{DyBa}_2\text{Cu}_3\text{O}_{7-\delta}$  and presence of intergranular phases and small precipitates in the grains. It is worth mentioning the observation of dislocations in the majority of grains. These dislocations can act as pinning centres.

Microanalysis was carried out in a SEM on bulk samples mechanically polished with surfaces. The results were compared with those reported above for  $x = 0.2$ . The two sets of values are in fair agreement for all the samples studied, showing the reliability of the results.

Another remarkable fact is the absence of silver in the grains for (A) and (C) samples, whatever the doping level. It appears that silver has no reactivity with the DyBCO lattice when it is already formed; Ag does not tend to expel Cu from its sites and to replace it. Even in (C) samples where Ag was present during the formation of the 123 lattice, Ag is never found in the grains, confirming the above conclusion and showing that it is easier to form  $\text{DyBa}_2\text{Cu}_3\text{O}_{7-\delta}$  than  $\text{DyBa}_2\text{Cu}_{3-x}\text{Ag}_x\text{O}_y$  when the ratio of Dy:Ba:Cu is exactly 1:2:3 even in presence of an important amount of Ag. So in the case of added samples (A) and (C), silver fills the pores and resides in the grain boundaries which are cleaner (free of second phases) than those of (S) samples.

A systematic statistical study of grain boundaries was performed in an attempt to correlate their distribution to the observed change in  $J_c$ . On each sample 50 consecutive boundaries were observed and characterized by bright field tilting imaging in TEM. Repetitive analyses on a test sample indicate a precision of  $\leq 6\%$  for the counting rate. The results are represented in figure 10. For S samples, it was observed that the number of dirty boundaries is much higher than for A samples. For higher concentrations it was not possible to carry out a statistical study on these samples

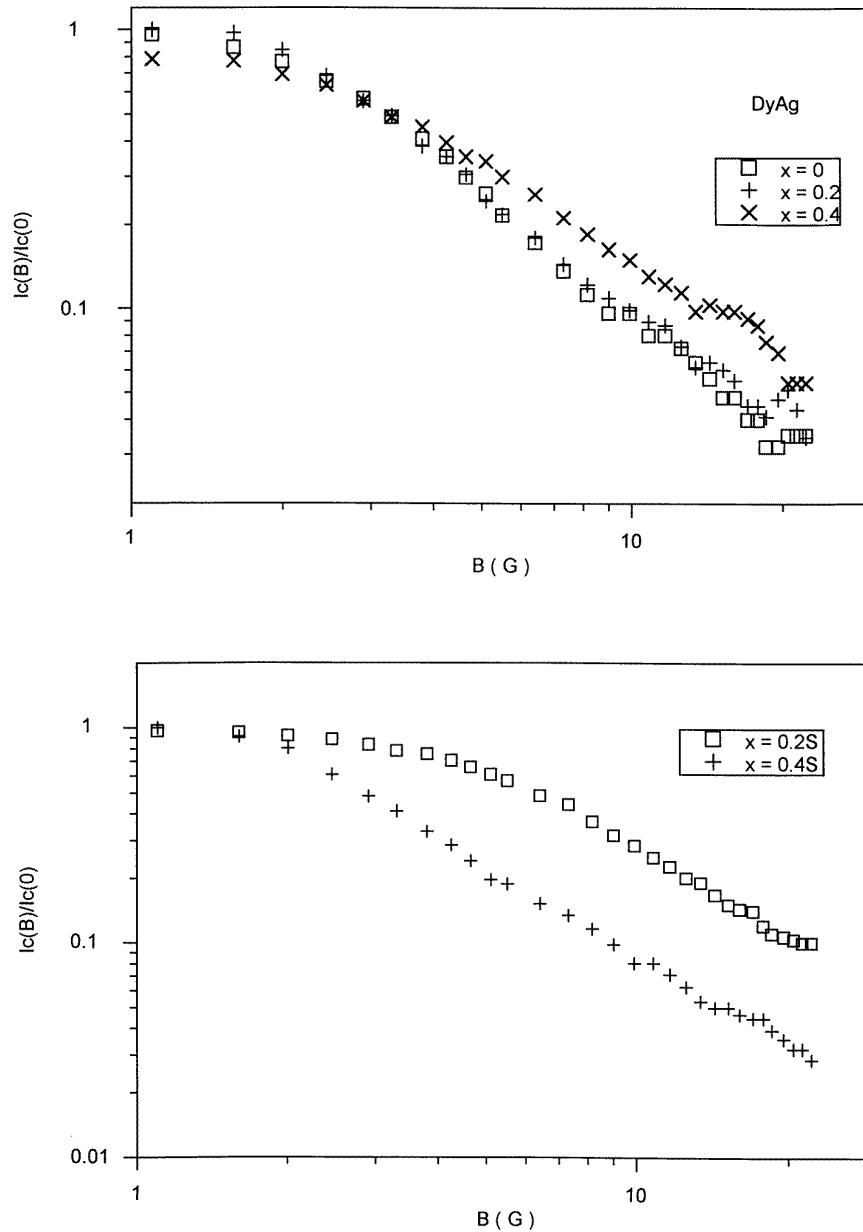


**Figure 8.** Transport critical current density at 77 K versus applied magnetic field in a logarithmic scale: (a) A ( $0 \leq x \leq 0.4$ ) samples; (b) S ( $0.2 \leq x \leq 0.4$ ) samples.

**Table 2.** Average concentration of silver in the grains measured by EDX in TEM and in SEM for substituted samples for all doping level.

Nominal Ag concentration $x$	Actual Ag concentration in the grains
0.05	< limit of detection
0.1	0.06
0.2	0.10
0.4	0.12

since they are too heterogeneous to allow a systematic survey of the boundaries

On the samples with Ag added, it was found that the ratio of clean boundaries remain between 16 and 26% for  $0 \leq x \leq 0.4$ . Moreover, clean boundaries are

favourable for transmitting the supercurrent only whenever the orientation relationships between adjacent crystals are suitable. This means that CuO<sub>2</sub> planes should remain parallel without rigid body translation between the two crystals (tilt boundaries) or that a common direction

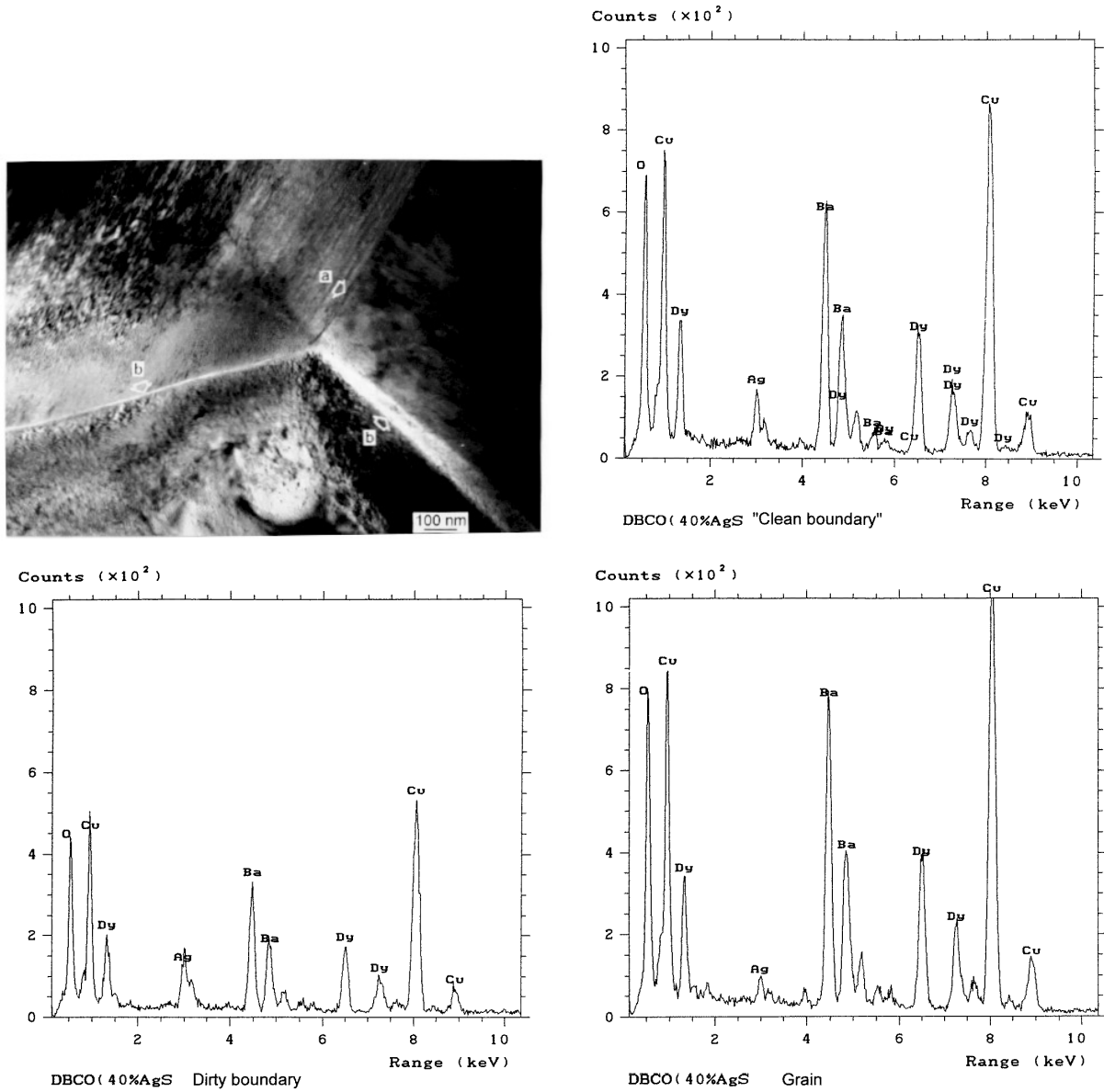


**Figure 9.** EDX spectra and corresponding micrograph in TEM for an  $x = 0.4S$  sample on (a) a clean boundary, (b) a dirty boundary, (c) a grain. All the constituent elements are identified on the EDX spectra.

contained in the  $\text{CuO}_2$  plane should exist between these crystals (twist boundaries). Consequently only 50% or less of clean boundaries could be considered as favourable. Thus the number of clean boundaries which attenuate the supercurrent slightly should be small and close to or lower than the percolation threshold ( $\approx 12\%$ ) [28]. Therefore the transmission of the supercurrent is likely to be ensured not only by specific clean boundaries but also by a fraction of thin-film-coated boundaries. Furthermore, it is seen that the number of intergranular thin films decrease when 10% Ag is added, and even more so when Ag is substituted.

Therefore, to understand the behaviour of boundaries in relationships with the microstructure and the resulting property of the ceramic, one must examine in detail the Ag distribution along boundaries. Table 3 gives the indicative values of Ag concentration obtained in TEM with the 20 nm

**Table 3.** Percentage of atomic Ag in ‘clean boundaries’ and in grains for (S) and (A) samples as a function of doping level.

x	S samples		A samples	
	Clean boundaries	Grains	Clean boundaries	Grains
0.1	2	1	1	$\leq 0.2$
0.2	3.6	1.65	1	$\leq 0.2$
0.4	6.6	2	1.5	$\leq 0.2$

probe on ‘clean’ boundaries for the different samples

It is inferred that the segregation at boundaries is much higher for S than for A samples (ratio 2 to 4). In the latter  $J_c$  increases when Ag is added whereas in the former it

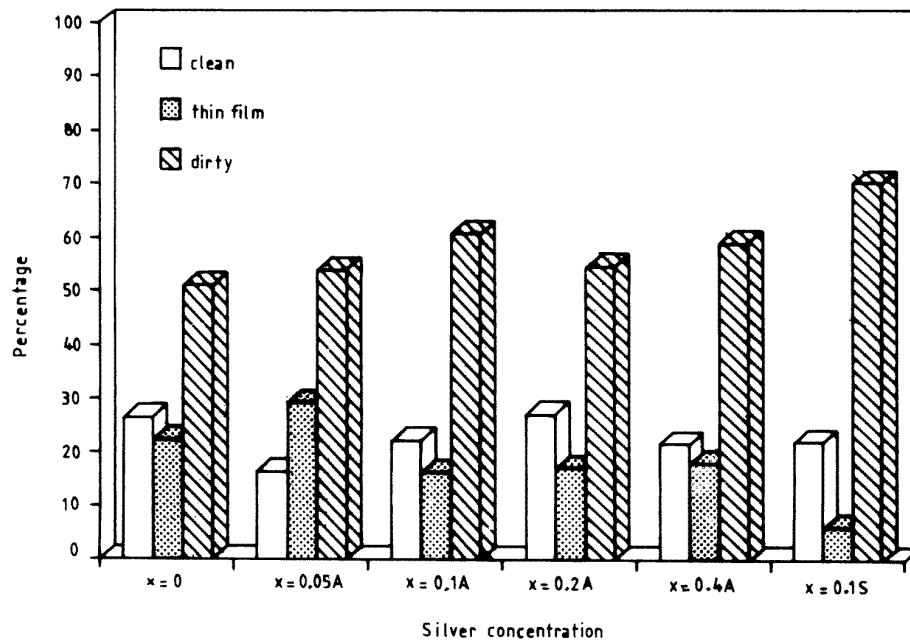


**Figure 10.** Histogram showing the distribution of clean, thin-film-coated and dirty grain boundaries for undoped, A ( $0.05 \leq x \leq 0.4$ ) and S ( $x = 0.1$ ) samples.

is the reverse. The decrease in  $J_c$  for S sample results from this strong segregation. As a consequence these 'clean' boundaries exhibit a weak link behaviour since the segregation width is likely to be large (a few nm) and gives rise to a strong attenuation of the supercurrent. On the contrary for A samples this segregation width remains sufficiently narrow to limit this attenuation. The value of  $J_c$  doubles when  $x$  goes from 0.2 to 0.4. It is seen from the histogram that this increase is by no means due to a diminution of the ratio of dirty boundaries. It is deduced that weak junctions at clean boundaries do strengthen when silver segregation increases slightly. These junctions weaken as soon as this segregation reaches a threshold which corresponds to  $x = 0.2$  for S samples and probably for  $x > 0.4$  for A samples. Moreover, the increasing proportion of dirty boundaries creates SIS junctions which impede the percolation on the A samples.

## 5. Conclusion

The superconducting properties ( $R-T$ ,  $I-V$  and  $J_c-B$ ) were correlated with a systematic characterization of the microstructure of grain boundaries, through TEM observation and local chemical analysis by EDX on DyBa<sub>2</sub>Cu<sub>3</sub>O<sub>7-δ</sub> sintered ceramics submitted to different types of Ag doping. The results shed light on the apparent contradictory data reported in the literature.

Silver does not exhibit reactivity with DyBCO 123. When added to the presynthesized DyBa<sub>2</sub>Cu<sub>3</sub>O<sub>7-δ</sub> or to the stoichiometric precursor powder, Ag does not enter into the '123' lattice; it is segregated in clean grain boundaries and precipitated as pure Ag metallic phase.  $J_c(B)$  data showed that all the samples behave as granular materials, i.e. that the current is limited by weak link junctions (SNS or SIS

junctions). The distinct enhancement in  $J_c$  with doping is attributed to an improvement of the weak link behaviour caused by Ag segregation in the grain boundaries which strengthens the weak links and not to an increased ratio of clean boundaries. The width of these boundaries remains sufficiently narrow to allow intergranular coupling and the percolation of the supercurrent.

In the attempt to substitute Ag for Cu, it was shown that Ag goes on the Cu sites only if they are vacant. The amount of silver incorporated in the lattice depends on the nominal Ag concentration. It is always less than this latter concentration and the maximum value is limited to approximately 0.12 (for  $x = 0.4$ ). This substituting behaviour of Ag leads to a Cu-deficient ceramic. The decrease in  $J_c$  for  $x \geq 0.2$  could be explained by an excessive Ag segregation at grain boundaries giving rise to wide junctions as well as by an increased proportion of second phases which impede the transmission of the supercurrent.

## References

- [1] Pavuna D, Berger H, Tholence J L, Affronte M, Sangines R, Dubas A, Bugnon Ph and Vasey F 1988 *Physica C* **153-5** 1339
- [2] Dwir B, Affronte M and Pavuna D 1989 *Physica C* **162-4** 351
- [3] Jung J, Mohamed M A K, Cheng S C and Franck J P 1990 *Phys. Rev. B* **42** 6181
- [4] Sen D, Bhattacharya D, Ghatak S K and Chopra K L 1991 *Bull. Mater. Sci.* **14** 927
- [5] Lee D and Salama K 1990 *Japan. J. Appl. Phys.* **29** L2017
- [6] Xia J A, Ren H T, Zhao Y, Andrikidis C, Munroe P R, Liu H K and Dou S X 1993 *Physica C* **215** 152
- [7] Lee D F, Chaud X and Salama K 1991 *Physica C* **181** 81
- [8] Kao Y H *et al* 1990 *J. Appl. Phys.* **67** 353

- [9] Joo J, Singh J P, Poeppel R B, Gangopadhyay A K and Mason T O 1992 *J. Appl. Phys.* **71** 2351
- [10] Weinberger B R, Lynds L, Potrepka D M, Snow D B, Burila C T, Eaton H E Jr, Cippoli R, Tan Z and Budnick J I 1989 *Physica C* **161** 91
- [11] Gangopadhyay A K and Mason T O 1991 *Physica C* **178** 64
- [12] Lin J J, Chen T-M, Yao Y D, Chen J W and Gou Y S 1990 *Japan. J. Appl. Phys.* **29** 497
- [13] Souletie B, Guillot M, Lejay J and Tholence J L 1991 *Solid State Commun.* **78** 717
- [14] Koslowski G, Rele S, Lee D F and Salama K 1991 *J. Mater. Sci.* **26** 1056
- [15] Pavuna D, Berger H, Affronte M, Van der Mass J, Capponi J J, Guillot M, Lejay P and Tholence J L 1988 *Solid State Commun.* **68** 535
- [16] Misra D S, John B, Pinto R, Mombasawala L S and Palmer S B 1995 *Physica C* **248** 276
- [17] Wang M J, Ling D C, Lin J L, Wu M K and Chi C C 1991 *Physica C* **185-9** 2417
- [18] De U, Natarajan S and Seibt E W 1991 *Physica C* **183** 83
- [19] Deslandes F, Raveau B, Dubots P and Legat D 1989 *Solid State Commun.* **71** 407
- [20] Taylor C R and Greaves C 1994 *Physica C* **235-40** 853
- [21] Zhang Ch, Kulpa A and Chaklader A C D 1995 *Physica C* **252** 67
- [22] Kao C H, Shine Y S, Sheen S R and Wu M K 1993 *Physica C* **205** 186
- [23] Ekin J W *et al* 1987 *J. Appl. Phys.* **62** 4821
- [24] Bednorz J G and Müller K A 1986 *Z. Phys. B* **64** 189
- [25] Clemm J R 1988 *Physica C* **153-5** 50
- [26] Peterson R L and Ekin J W 1988 *Phys. Rev. B* **37** 9848
- [27] Peterson R L and Ekin J W 1989 *Physica C* **157** 325
- [28] Sarma C, Schindler G, Haase D G, Koch C C, Kingonand A I and Goyal A 1995 *Physica C* **244** 287
- [29] Shante V K S and Kirpatrick S 1971 *Adv. Phys.* **20** 325